Pharmacokinetic Analysis Of The Blood-Brain Barrier Transport Of ^{125}I-Aβ40 In Wild Type And Alzheimer's Disease Transgenic Mice (APP,PS1) And Its Implications For Amyloid Plaque Formation

Karunya K. Kandimalla, Geoffry L. Curran, Silvina S. Holasek, Emily J. Gilles, Thomas M. Wengenack, and Joseph F. Poduslo

Molecular Neurobiology Laboratory

Departments of Neurology, Neuroscience, and Biochemistry/Molecular Biology

Mayo Clinic College of Medicine, Rochester, MN 55905 (*KK, GC, SH, EG, TW, JP*)

Running title: Pharmacokinetics analysis of the BBB transport of ^{125}I-Aβ40

Corresponding author: Joseph F. Poduslo

Address: Mayo Clinic College of Medicine, 200 First Street SW, Rochester, MN55905

Phone: (507) 284 1784

Fax: (507) 284 3383

Email: poduslo.joseph@mayo.edu

Number of text pages: 23

Number of tables: 5

Number of figures: 5

Number of references: 23

Number of words in the abstract: 249

Number of words in the introduction: 538

Number of words in the discussion: 1727

Abbreviations:

AD, Alzheimer's disease; Aβ40, unlabeled amyloid beta 40; ^{125}I-Aβ40, amyloid beta 40 labeled with ^{125}I; APP, amyloid precursor protein; PS1, presenilin 1; WT, wild type; BBB, blood brain barrier; CSF, cerebrospinal fluid; IV, intravenous; BSA, bovine serum albumin; BCA, Bicinchoninic acid protein assay reagent ; TCA, trichloroacetic acid; V_p, residual brain region plasma volume; PS, cerebrovascular permeability coefficient-surface area product ; KRB, Kreb's Ringer bicarbonate buffer; DMEM, Dulbecco's modified eagle medium; 2,4-DNP, 2,4-dinitrophenol; V_{ss}, steady state volume of distribution; AUC, area under the plasma concentration curve; Cl, clearance.

Section option: Absorption, Distribution, Metabolism & Excretion

ABSTRACT

Amyloid plaques are formed in the extracellular space of Alzheimer's disease (AD) brain due to the accumulation of amyloid β proteins (Aβ) such as Aβ40. The relationship between Aβ40 pharmacokinetics and its accumulation within and clearance from the brain in both wild type (WT) and AD transgenic mice (APP,PS1) was studied to understand the mechanism of amyloid plaque formation and the potential use of Aβ40 as a probe to target and detect amyloid plaques . In both WT and APP,PS1 mice, the ^{125}I- Aβ40 tracer exhibited bi-exponential disposition in plasma with very short first and second phase half-lives. The ^{125}I-Aβ40 was significantly metabolized in the liver >>> kidney > spleen. Co-administration of exogenous Aβ40 inhibited the plasma clearance and the uptake of ^{125}I-Aβ40 at the BBB in WT animals but did not affect its elimination from the brain. The ^{125}I-Aβ40 was shown to be metabolized within and effluxed from the brain parenchyma. The rate of efflux from APP,PS1 brain slices was substantially lower compared to WT brain slices. Since the Aβ40 receptor at the BBB can be easily saturated, the blood-to-brain transport of Aβ40 is less likely to be a primary contributor to the amyloid plaque formation in APP,PS1 mice. The decreased elimination of Aβ40 from the brain is most likely responsible for the amyloid plaque formation in the brain of APP,PS1 mice. Furthermore, inadequate targeting of Aβ40 to amyloid plaques despite its high BBB permeability is due to the saturability of Aβ40 transporter at the BBB and its metabolism and efflux from the brain.

INTRODUCTION

Development of amyloid plaques in the extracellular space of the brain parenchyma is considered a primary event in the pathogenesis of Alzheimer's disease (AD) (Selkoe, 2001). Amyloid plaques consist predominantly of the amyloid beta (Aβ) proteins, Aβ40 and Aβ42, which are produced continuously by cells in the nervous system and peripheral tissues. The higher concentration of soluble Aβ accumulates over time in the brain extracellular space, polymerizes into insoluble fibrils, and eventually forms amyloid plaques (Craft et al., 2002; Cirrito et al., 2003). Studies in AD patients indicated increased levels of peripherally circulating Aβ (Kuo et al., 1999; Matsubara et al., 1999). DeMattos and collegues (2002) suggested that Aβ in plasma and CSF exist in equilibrium, which is controlled by a novel, yet unknown mechanism, that shifts toward the brain during plaque development. Zlokovic (2004) proposed that the Aβ equilibrium between plasma and CSF is regulated at the blood brain barrier (BBB) by an influx receptor (RAGE, receptor for advanced glycation end products) and an efflux receptor (LRP-1, low-density lipoprotein receptor-related protein).

In the recent years, substantial effort has focused on the development of a pre-mortem diagnosis of AD, which involves detection of the plaques using various imaging techniques such as magnetic resonance imaging (MRI) and positron emission tomography (PET). MRI used in conjunction with a contrast agent can resolve individual plaques and has the capability of differentiating plaques from other interfering structures such as blood vessels, myelinated fibers, and intracranial structures (Poduslo et al., 2002). Of the MRI contrast agents that are currently being developed for imaging amyloid plaques, the most notable is the amyloid protein itself, mostly Aβ40

(Wengenack et al., 2000a; Lee et al., 2002; Poduslo et al., 2002; Wadghiri et al., 2003; Poduslo et al., 2004). ^{125}I-Aβ40 was reported to have high binding affinity to the amyloid plaques in human and double transgenic AD mouse (APP,PS1) brain slices in vitro and high in vivo permeability at the BBB; however, the plaque targeting ability of ^{125}I-Aβ40 after IV injection in AD transgenic mice was low (Wengenack et al., 2000a). Hence, methods such as modifying the protein so that it can be actively transported across the BBB have been employed to increase the targeting of Aβ40 after intravenous injection (Wengenack et al., 2000a; Poduslo et al., 2002; 2004). The inadequate targeting of Aβ40 to amyloid plaques despite its high permeability at the BBB could be due in part to:

1) rapid elimination of Aβ40 from the systemic circulation which leads to a reduction in its concentration at the BBB

2) inadequate transcytosis across the capillary endothelium,

3) competing high level of efflux from the brain parenchyma, or

4) metabolism in the brain or uptake by various cells which can deplete Aβ40 concentrations from the extracellular space.

Some of these questions are addressed in the present study using mechanism-based pharmacokinetic experiments employing a tracer (^{125}I-Aβ40) in both wild type (WT) and AD transgenic mice (APP,PS1). Our investigation also addresses questions regarding the relationship between endogenous Aβ40 and the kinetics of Aβ accumulation and clearance from the brain. Such information is not only helpful in elucidating the disease pathology but also in optimizing the delivery of diagnostic probes derived from Aβ (Poduslo et al., 2004).

METHODS

Animals. The double transgenic mice were bred in our mice colony at Mayo. Hemizygous transgenic mice (mouse strain: C57B6/SJL; I.D. No. Tg2576) expressing mutant human amyloid precursor protein (APP_{695}) (Hsiao et al., 1996) were mated with a second strain of hemizygous transgenic mice (mouse strain: Swiss Webster/B6D2; I.D. No. M146L6.2) expressing mutant human presenilin 1 (PS1) (Holcomb et al., 1998). These double transgenic mice have been shown to exhibit an accelerated phenotype with amyloid deposits and behavioral deficits by 12 weeks of age (Holcomb et al., 1998; Wengenack et al., 2000b). Wild type (WT) mice (B6/SJL) were obtained from The Jackson Laboratory (Bar Harbor, ME) at 6-8 weeks of age and were the same background strain as the transgenic mice. The animals were housed in a virus-free, indoor, light-and temperature-controlled barrier environment and were provided ad libidum access to food and water. All procedures with animals were in strict accordance with the NIH "Guide for the Care and Use of Laboratory Animals" and approved by the Mayo Institutional Animal Care and Use Committee.

Synthesis of Aβ40. Human Aβ40 was synthesized by the Mayo Protein Core Facility (Rochester, MN) on an ABI 433A Peptide Synthesizer (PE Biosystems, Foster City, CA), using standard solid phase methods and procedures. Each peptide was purified by reverse phase HPLC on a Jupiter C18 column (250 x 21.2 mm, 15µ; Phenomenex, Torrance, CA) in 0.1% trifluoroacetic acid (TFA)/water with a 50 min gradient from 10-70% acetonitrile/0.1% TFA. The integrity of the protein was verified by electrospray ionization (ESI) mass analysis on a Perkin/Elmer Sciebx API 165 Mass Spectrometer (PE Biosystems, Foster City, CA). Protein concentration was determined using a

bicinchoninic acid protein assay reagent (BCA) kit (Pierce Chemical Company, Rockford, IL) and bovine serum albumin standard.

Radioiodination of Proteins. Career-free $Na^{125}I$ and $Na^{131}I$ were obtained from Perkin-Elmer Analytical Sciences (Boston, MA). Human Aβ40 (500 µg) and bovine serum albumin (BSA) (500 µg) were labeled with ^{125}I and ^{131}I, respectively, using the chloramine-T procedure as described previously (Poduslo et al., 1994). Free radioactive iodine was separated from the radiolabeled protein by dialysis against 0.01 M phosphate buffered saline at pH 7.4 (Sigma-Aldrich Co., St. Louis, MO). Purity of the radiolabeled proteins was determined by trichloroacetic acid (TCA) precipitation. The radiolabeled protein was determined to be acceptable if the TCA precipitable counts were greater than 95% of the total counts. The final radioactivity associated with ^{125}I labeled Aβ40 was determined to be 4 mCi/mg of protein.

Aβ40 Pharmacokinetics Studies. Before the beginning of experiment each mouse was weighed (WT = 18-21 g; APP,PS1 = 20-23 g), and the femoral vein and artery were catheterized under general anesthesia (isoflurane = 1.5% and oxygen = 4 l/min). The ^{125}I-Aβ40 (100 µCi, 100 µl) was administered intravenously in the femoral vein. Blood was sampled (20 µl) from the femoral artery at various intervals. At the end of the experiment, an aliquot of ^{131}I-BSA (100 µCi, 100 µl) was injected to serve as a measure of residual plasma volume (V_p). One minute following the ^{131}I-BSA injection, the final blood sample was collected, and the animal was sacrificed. The blood samples diluted to a volume of 100 µl using normal saline were centrifuged, and the supernatant was obtained. Following TCA precipitation, the samples were assayed for ^{125}I and ^{131}I radioactivity in a two-channel gamma counter (Cobra II, Packard). The measured

activity was corrected for the background and crossover of ^{131}I activity into the ^{125}I channel.

The plasma pharmacokinetics of ^{125}I-Aβ40 was determined by collecting serial blood samples (20 µl) from the femoral artery over a period of 15 min at time points of 0.25, 1, 3, 5, 10 and 15 min. The accumulation of ^{125}I-Aβ40 in the peripheral organs such as liver, kidney and spleen was determined by perfusing the animals with PBS at the end of the experiment. The linearity of ^{125}I-Aβ40 disposition was determined by repeating the experiment by co-administering 1 or 2 mg of cold Aβ40 with 100 µCi of ^{125}I-Aβ40.

The brain uptake studies of ^{125}I-Aβ40 were conducted by collecting serial blood samples (20 µl) from the femoral artery over a period of 15 min at time points 0.25, 1, 3, 5, 10, 15 min. At the end of the experiment, the brain of the animal was removed from the cranial cavity, dissected into the anatomical regions, cortex, caudate putamen, hippocampus, thalamus, brain stem, and cerebellum, and assayed for ^{125}I and ^{131}I radioactivity. The brain regions were lyophilized and dry weights were determined with a microbalance and converted to wet weights using wet weight/dry weight ratios determined previously. The saturability of ^{125}I-Aβ40 transport at the blood brain barrier was determined by co-administering 0.5, 1, or 2 mg of cold Aβ40 with 100 µCi of ^{125}I-Aβ40.

To determine the influence of high circulating levels of Aβ40 on the elimination of ^{125}I-Aβ40 from the brain, 100 µCi of ^{125}I-Aβ40 was administered to the animal intravenously followed by 4 IV bolus injections of 0.5 mg cold Aβ40 at 15 (t_{max} of ^{125}I-Aβ40 in the brain), 30, 45 and 60 min intervals. Blood samples were collected over a

period of 60 min at time points 0.25, 1, 3, 5, 10, 15, 30, 45 and 60 min. At the end of 90 min, ^{131}I-BSA was administered; the animal was sacrificed a minute later to obtain the brain regions, which were assayed for ^{125}I and ^{131}I radioactivity as described above.

Metabolism of ^{125}I-Aβ40. To determine the metabolism of ^{125}I-Aβ40 in the plasma of WT or AD transgenic animals, 0.1 µCi of ^{125}I-Aβ40 was added to 350 µl of plasma and incubated at 37 ^{o}C. Aliquots from the mixture (20 µl) were taken at regular intervals up to 60 min, and the amount of intact ^{125}I-Aβ40 was determined by TCA precipitation. The metabolism of ^{125}I-Aβ40 in the presence of brain, liver, kidney and spleen slices was determined by obtaining the organs from WT and AD transgenic mice following perfusion with PBS. The organs were weighed, cut into 1mm thick slices using a tissue slicer (Stoelting Co. Wood Dale, IL), and placed in Dulbecco's modified eagle medium (DMEM) (Invitrogen Corporation, Grand Island, NY) pre-warmed to 37°C. ^{125}I-Aβ40 (0.1 µCi) was added to the medium containing tissue slices and maintained at 37°C under 5% CO_2 for the entire length of the experiment. Aliquots (20 µl) of the medium were obtained at regular intervals and assayed for the intact protein using TCA precipitation method.

Efflux of ^{125}I-Aβ40 from brain slices. WT and APP,PS1 transgenic mice were killed by decapitation under general anesthesia. The brains were rapidly removed, washed with PBS, and cut into 1 mm thick cortical slices, containing hippocampus, using the tissue slicer. After equilibrating in oxygenated (95% O_2 / 5% CO_2) Krebs-Ringer Bicarbonate buffer (KRB) for 15 min at 37°C, each slice was incubated in 1 ml donor solution (0.6 µCi of ^{125}I-Aβ40 in 1ml of KRB) at 37°C for 30 min. The loaded brain slices were washed with KRB, and the efflux rate of ^{125}I-Aβ40 from each brain slice was determined

9

by incubating it in 5 ml of receiver medium (KRB or KRB + 1mM 2, 4-dinitrophenol) at 37°C. The receiver medium was replaced every 30 min to maintain sink conditions. One brain slice was sampled at various time intervals and assayed for ^{125}I radioactivity.

Data Analysis. The Aβ40 plasma concentration profile following a single intravenous bolus dose of ^{125}I-Aβ40 was best described by a biexponential disposition function $C(t) = Ae^{-\alpha t} + Be^{-\beta t}$, (eq. 1) where C(t) = ^{125}I-Aβ40 (µCi) / ml of plasma, A and B are the intercepts and α and β are the slopes of the biexponential curve. Pharmacokinetic parameters were estimated by nonlinear curve fitting using Gauss-Newton (Levenberg and Hartley) algorithm and iterative reweighting (WinNonlin$^{®}$ Professional, version 4.1, Mountain view, CA). Secondary parameters such as the C_{max} (maximum plasma concentration), the first ($t_{1/2(\alpha)}$) and second phase ($t_{1/2(\beta)}$) half-lives, the plasma clearance (Cl), the steady-state volume of distribution (V_{ss}), and area under the plasma concentration curve (AUC) were also calculated using WinNonlin. The mean values of controls and treatments were compared by Student's t-test using GraphPad Prism version 3.03 (GraphPad Software, San Diego, CA).

The residual brain region plasma volume (V_p, µl/g) and the cerebrovascular permeability-surface area product (PS) values were calculated as described previously by Poduslo (1993).

$$V_p = \frac{q_p \times 10^3}{C_v \times WR}, \quad \text{(eq. 2)}$$

where q_p is the ^{131}I-BSA content (cpm) of tissue, C_v is the ^{131}I-BSA concentration (cpm/ml) in plasma, W is the dry weight (g) of the brain region, and R is the wet weight / dry weight ratio for mice of a defined age group. From the total ^{125}I-Aβ40 content (q_T)

(cpm) of the brain region, the amount of ^{125}I-Aβ40 that enters the brain region extravascular space (q) (cpm/g) is calculated as

$$q = \frac{q_T}{WR} - \frac{V_p C_a}{10^3}, \text{ (eq. 3)}$$

where C_a is the final ^{125}I-Aβ40 concentration (cpm/ml) in plasma. The PS (ml/g/s) at the BBB is calculated as

$$PS = \frac{q(t)}{\int_0^t C_p dt}, \text{ (eq. 4)}$$

where t is the circulation time, q(t) is the extravascular ^{125}I activity in the brain region at time t, and $\int_0^t C_p dt$ is the plasma concentration time integral of ^{125}I-Aβ40.

The rate of ^{125}I-Aβ40 efflux (k) from the brain slices in vitro was determined by curve-fitting (one-phase exponential decay model) the amount of radioactivity retained in the brain slices versus time using GraphPad Prism version 3.03 as follows.

$$Y = Y_o\, e^{-kt} + \text{plateau (eq. 5)}$$

where Y_o is the amount of radioactivity (cpm) in the brain slice at 0 min, k is the decay rate constant and t is the time in minutes. The adequacy of fit was determined by F test.

The PS values of ^{125}I-Aβ40 was plotted versus the log concentration (log C) of Aβ40, and the inhibitor concentration 50% (IC$_{50}$) of Aβ40 in various brain regions were calculated by fitting one-site competitive binding equation to the data using GraphPad Prism version 3.03:

$$PS = PS_{min} + \frac{(PS_{max} - PS_{min})}{(1 + 10^{\log C - \log IC50})} \qquad \text{(eq. 6)}$$

11

where PS_{max} is the maximum PS value, which was obtained at the lowest Aβ40

concentration. PS_{min} is the minimum PS value obtained at the highest Aβ40

concentration.

RESULTS

Recent reports have suggested that Aβ40 exhibits bidirectional transport between the peripheral circulation and brain via the BBB (Shibata et al., 2000; Deane et al., 2003). According to Zlokovic (2004), such a bidirectional transport regulates the Aβ40 equilibrium between CNS and peripheral circulation and contributes to the formation of amyloid plaques in the brain parenchyma. If peripherally circulating Aβ40 can so directly impact AD pathogenesis, then it becomes important to study the plasma pharmacokinetics of ^{125}I-Aβ40 in WT and AD mice. Differences in peripheral distribution and elimination between the two strains could have a profound influence on plasma and brain steady state Aβ concentrations, as well as on the time course of brain [125]I- Aβ40 concentration after IV administration. The information obtained from such a comparative study could help optimize Aβ40 delivery (or its derivatives) as a diagnostic probe and elucidate the physiological parameters responsible for plaque formation in AD mice.

[125]I-Aβ40 plasma pharmacokinetics and metabolism. Following IV administration, the ^{125}I-Aβ40 concentration in the plasma of WT as well as APP,PS1 mice declined rapidly exhibiting a bi-exponential disposition with short first ($t_{1/2,\alpha}$) and second phase ($t_{1/2,\beta}$) half-lives (Fig. 1A, Table 1). The plasma pharmacokinetic profile of ^{125}I-Aβ40 in 8 week APP,PS1 mice (no amyloid plaque formation), was significantly different from that of the 8 week WT mice. However, this difference was not statistically significant when the animals were 24 weeks old (Fig. 1B, Table 1), an age with substantial amyloid burden (Wengenack et al., 2000b). While no significant differences in the plasma pharmacokinetic parameters were observed between 8 and 24 week old WT mice, significantly lower clearance and higher AUC was observed in 24 week old

13

APP,PS1 mice compared to that of 8 week old mice (Table 1). These differences are most likely due to the increased Aβ40 levels with age in APP,PS1 mice that could saturate peripheral elimination.

A substantial amount of ^{125}I-Aβ40 was found in the liver, kidney and spleen of both WT and APP,PS1 animals perfused with PBS at the termination of the experiment. The accumulation of ^{125}I-Aβ40 was higher in the kidney than in the liver or spleen. Moreover, no significant differences in the accumulation of ^{125}I-Aβ40 in these organs was observed between WT and APP,PS1 animals. To investigate the role of peripheral metabolism on the rapid elimination of ^{125}I-Aβ40 from the systemic circulation, in vitro metabolism studies in the presence of plasma, liver, kidney and spleen obtained from WT and APP,PS1 mice were conducted. Although the ^{125}I-Aβ40 metabolism in the plasma was slightly higher than the degradation in DMEM at 37 ^{o}C, less than 10% of the initial amount of ^{125}I-Aβ40 was degraded in 60 min (Fig. 2). The metabolism of ^{125}I-Aβ40 in the liver slices, however, was so rapid that Aβ40 was degraded substantially before initial sample (t = 0 min) could even be obtained, and proceeded to near completion by 60 min (Fig. 2). The metabolism in the APP,PS1 mouse peripheral tissues was not significantly different from that of WT mouse tissues. However, the ^{125}I-Aβ40 metabolism in the brain slices of APP,PS1 mice is significantly lower compared to that in wild type brain slices(Fig. 2).

To determine if the elimination of ^{125}I-Aβ40 from the peripheral circulation is saturable, the plasma kinetics of ^{125}I-Aβ40 was studied by co-administering various amounts of unlabeled Aβ40 (0.125-4 mg). When 0.125 mg of Aβ40 was co-administered with 100 μCi ^{125}I-Aβ40, no significant changes in the plasma pharmacokinetic

14

parameters were observed (Table 2). Upon co-administration of 1, 2 or 4 mg of Aβ40, the pharmacokinetic parameters of clearance and V_{ss} of ^{125}I-Aβ40 decreased significantly where as the AUC increased significantly (Table 2).

^{125}I-Aβ40 brain uptake. Upon intravenous administration in 24 week old WT mice, ^{125}I-Aβ40 showed rapid brain uptake (t_{max} ~ 15 min) (Fig. 3). ^{125}I-Aβ40 pharmacokinetic profile in the brain was substantially different from that of the plasma. Elimination of ^{125}I-Aβ40 from the brain was not as rapid as it was from the plasma.

To verify if the uptake of ^{125}I-Aβ40 at the BBB is receptor-mediated, various amounts of unlabeled Aβ40 was co-administered along with ^{125}I-Aβ40 in 24 week old WT mice. When 28.8 nM (0.125 mg) of Aβ40 was co-administered, the decrease in the PS values of ^{125}I-Aβ40 in all brain regions was statistically significant ($p<0.05$) (Table 3). Further increments of unlabeled Aβ40 to 115.4 nM (0.5 mg), 231 (1 mg), 462 (2 mg) or 924 nM (4mg) resulted in a non-linear decrease in the PS value (Fig. 4a). The IC_{50} values of ^{125}I-Aβ40 PS values in cortex, caudate putamen, hippocampus, thalamus, brain stem and cerebellum were 73.0, 58.2, 108.9, 49.9, 81.2 and 78.7 nM, respectively (Fig. 4b). The V_p values, however, did not change significantly with the co-administration of unlabeled Aβ40 (Table 3).

The PS values of ^{125}I-Aβ40 at the BBB in various brain regions of 8 and 24 week old APP,PS1 transgenic mice were significantly lower than that in age matched WT mice (Table 4). There was no significant difference in the V_p values of ^{125}I-Aβ40 in various brain regions except in hippocampus and brain stem (Table 4). These findings differ from that of our earlier report where no differences in the PS values of ^{125}I-Aβ40 between AD transgenic and normal mice were observed (Poduslo et al., 2001). In the

earlier study, we used ^{131}I-Aβ40 as vascular space marker, but in this study ^{131}I-BSA was used to estimate the V_p values of ^{125}I-Aβ40 in both WT and AD transgenic mice. Using the same protein labeled with a different isotope helps correct for potential artifacts such as nonspecific adherence to vessel walls and allows for an accurate estimation of residual brain plasma volume (V_p). However, further studies conducted in our lab demonstrated that rapid elimination of proteins such as Aβ40 (unpublished data), whose plasma concentrations are reduced by ~ 50% in 45 sec, can lead to an under estimation of PS values. Moreover, differences in the circulating levels of endogenous Aβ40 in WT and AD transgenic mice further confounds the determination of these parameters (Poduslo et al., 2001). Another reason for the differences between the two studies is the manner in which the blood samples were processed. In the former study, the TCA precipitation to quantify the intact protein was conducted on whole blood, whereas in the current study, the blood was diluted and centrifuged to remove cells and the TCA precipitation was conducted on the diluted plasma.

The APP,PS1 mice at the age of 6 months develop distinct plaques, mostly in the cortex and hippocampus (Wengenack et al., 2000). They also carry significantly higher levels of Aβ40 (13.9 pmol/ml) in the peripheral circulation compared to wild type mice (1.07 pmol/ml) (Poduslo et al., 2001). If one of the primary elimination pathways of Aβ40 from the brain involves efflux into peripheral circulation across the blood brain barrier via LRP1 located on the abluminal surface (Shibata et al., 2000), the higher levels of Aβ40 in the peripheral circulation of the transgenic mice could reduce Aβ40 efflux by saturating the efflux transporter. To investigate this hypothesis, a pharmacokinetic study based on the absorption and elimination profile of ^{125}I-Aβ40 in the extravascular brain

tissue (Fig. 3) was designed. A bolus dose of ^{125}I-Aβ40 was administered to WT mice intravenously starting at the t_{max} of ^{125}I-Aβ40 in the brain (~15 min), four IV bolus doses of unlabeled Aβ40, each 0.5 mg, was injected at 15 min intervals up to 60 min; the brain levels of ^{125}I-Aβ40 were then measured at the end of 90 min. Control experiments were performed on a similar set of three WT animals by injecting saline instead of unlabeled Aβ40. The assumptions behind this experiment were:

a) most of the uptake of ^{125}I-Aβ40 into endothelial cells or brain parenchyma takes place during the absorption phase (0-15 min).

b) If the efflux of the absorbed ^{125}I-Aβ40 from brain is inhibited by higher concentrations of Aβ40 (resulting from multiple bolus doses) on the luminal side, higher amounts of ^{125}I-Aβ40 remain in the brain compared to the control.

The amount of ^{125}I-Aβ40 in various brain regions of mice injected with unlabeled Aβ40 (treatment) was not significantly different from the amount present in the brain regions of mice injected with saline (control) (Table 5). No significant differences were found in the V_p values as well. These results suggest that the higher concentration of Aβ40 in the peripheral circulation does not influence the brain efflux of ^{125}I-Aβ40 significantly.

Efflux of ^{125}I-Aβ40 from brain slices. In the past, investigators have demonstrated that intracerebrally injected ^{125}I-Aβ40 was effluxed into CSF and blood (Ghersi-Egea et al., 1996; Shibata et al., 2000). While the mechanism of efflux is still not clear, it is reasonable to assume that the transport across the brain parenchyma plays a significant role in the efflux of ^{125}I-Aβ40 from brain. Hence the efflux rate of ^{125}I-Aβ40 from the brain slices of WT and APP,PS1 animals was determined in vitro. The efflux of

17

[125]I-Aβ40 from the brain slices of WT (in the presence and absence of 2,4-DNP) and APP,PS1 transgenic animals (24 weeks) were significantly different from each other (Fig. 5) (F-test, $p<0.0001$). The efflux rate of ^{125}I-Aβ40 from the WT mouse brain slices was 0.06 ± 0.01 min^{-1} and was significantly higher than that of brain slices obtained from APP,PS1 transgenic animals (0.02 ± 0.009 min^{-1}) (mean $\pm$ SEM). In the presence of a metabolic inhibitor like 2,4-DNP, which interferes with the energy metabolism, the efflux of ^{125}I-Aβ40 from the WT mouse brain slices was reduced to 0.02 ± 0.003 min^{-1} (mean $\pm$ SEM).

DISCUSSION

The objective of this work was to elucidate the role of ADME (absorption, distribution, metabolism and elimination) characteristics of Aβ40 in the plasma and brain of APP,PS1 mice. This objective was accomplished with the resulting conclusions:

i)   Accumulation of Aβ40 in the systemic circulation of APP,PS1 mice is not due to impaired plasma clearance.

ii)   Neither Aβ40 influx nor efflux across the BBB plays a pivotal role in the accumulation of Aβ40 in the brain.

iii)   Accumulation of Aβ40 in the brains of APP,PS1 animals is due to ineffective efflux in the brain parenchyma and/or reduced metabolism.

Our experiments demonstrated no major differences in the plasma pharmacokinetics or peripheral metabolism of ^{125}I-Aβ40 between WT and APP,PS1 animals. The high level of circulating Aβ40 in APP,PS1 animals could saturate the transporter at the BBB and hence contribute insignificantly to the amyloid plaque formation in the brain. Also, these kinetic experiments provided no direct evidence for the existence of Aβ40 efflux transport at the BBB. On the other hand, ^{125}I-Aβ40 efflux studies conducted in the brain slices, used as an vitro model for brain parenchymal transport demonstrated substantially higher efflux rate from WT brain slices compared to that of APP,PS1 brain slices. Moreover, the rate of ^{125}I-Aβ40 degradation in the presence of APP,PS1 brain slices is substantially lower compared to that of WT brain slices. The conclusions from our experimental studies that lead to these key findings are further elaborated below.

Following IV administration, our studies have demonstrated that the tracer ^{125}I-Aβ40 was eliminated rapidly from the plasma. Such rapid clearance of Aβ40 from the systemic circulation could adversely affect its permeability at the BBB and limits its utility as a diagnostic probe. The distribution and elimination half-lives of ^{125}I-Aβ40 in WT mice are lower than those reported in non-human primate model of cerebral β-amyloidosis (Mackic et al., 2002). Similar results are expected with AD transgenic mice used in this study, because they have higher plasma Aβ40 levels than the WT animals (Poduslo et al., 2001). The higher plasma levels of Aβ40 could saturate the receptors and/or enzymes involved with the distribution and metabolism of Aβ40, resulting in higher distribution and elimination half-lives. Surprisingly, ^{125}I-Aβ40 clearance and AUC were significantly higher in APP,PS1 mice (8 weeks) compared to that in 8 week old WT mice. However, at 24 weeks of age, when the peripherally circulating Aβ40 in APP,PS1 mice is 12 times higher than in WT mice (Poduslo et al., 2001), the ^{125}I-Aβ40 plasma profiles were similar.

To investigate the effect of higher endogenous plasma Aβ40 concentrations on the elimination of Aβ40 from the plasma, ^{125}I-Aβ40 was co-administered with various amounts of unlabeled Aβ40 into the systemic circulation of WT mice. In the presence of high plasma concentrations of Aβ40, the clearance and V_{ss} of ^{125}I-Aβ40 decreased significantly, which suggest that ^{125}I-Aβ40 exhibits non-linear disposition in the systemic circulation. In vitro metabolism studies conducted using WT and APP,PS1 mouse tissue slices indicated that ^{125}I-Aβ40 is substantially metabolized in liver and kidney. However, no significant difference in the extent of metabolism between WT and APP,PS1 animals

was observed. These results demonstrate, therefore, that the lower clearance of Aβ40 in 24 week old APP,PS1 mice compared to that in 8 week old animals is due to the higher circulating Aβ40 levels saturating the peripheral elimination. Despite the absence of any differences in the metabolism of Aβ40 in the peripheral tissues such as plasma, liver, kidney, and spleen of APP,PS1 and WT mice, the increase in the plasma levels of Aβ40 with age in APP,PS1 mice indicates that Aβ40 is replenished at a rate faster than it is removed from the peripheral circulation. Excess Aβ40 in the peripheral circulation could be due to over production by the peripheral tissues and/or probable continual efflux from the brain.

In order for Aβ40 in the peripheral circulation to directly contribute to the plaque formation in the brain parenchyma, it has to be transported across the BBB. Several investigators in the past have reported that Aβ40 is actively transported at the BBB (Zlokovic et al., 1993; Poduslo et al., 1997; 1999). Brain pharmacokinetic profile obtained in the present study demonstrated that ^{125}I-Aβ40 is absorbed at the cerebral vasculature very rapidly without any lag time, which is expected if the transport is receptor mediated. A decrease in the PS value of ^{125}I-Aβ40 in the presence of various amounts of unlabeled Aβ40 provides further evidence that ^{125}I-Aβ40 exhibits receptor mediated transport at the BBB.

Deane et al. (2003) claimed that RAGE mediates Aβ transport across the BBB and accumulation in brain. They reported that RAGE is upregulated in cerebral vasculature of patients with Alzheimer's disease and in AD mouse model and hypothesized that inhibition of RAGE at the BBB may limit accumulation of Aβ in the brain. If the Aβ40 transport across the BBB is mediated primarily by RAGE, we would

expect to see higher ^{125}I-Aβ40 PS values in APP,PS1 mice compared to WT mice consistent with the RAGE upregulation . On the contrary, the current study demonstrates that the PS value of ^{125}I-Aβ40 is significantly lower in APP,PS1 mice compared to WT mice most likely due to the saturation of uptake receptors at the BBB with increasing levels of Aβ40 in the plasma.

Although researchers in the past have reported that ^{125}I-Aβ40 have reasonable permeability at the BBB in APP,PS1 mice and non-human primates (Poduslo et al., 1999; Mackic et al., 2002), our laboratory and others have realized that the transport of Aβ40 into brain parenchyma is poor (Wengenack et al., 2000a; Lee et al., 2002; Poduslo et al., 2002; Wadghiri et al., 2003). The PS value represents the rate at which a protein is transferred from the blood to the endothelial cell, but offers no information on the amount of protein delivered to the brain parenchyma. Hence, care must be taken not to over interpret this parameter. Wengenack et al. (2000a) reported that no detectable signal due to ^{125}I-Aβ40 was observed on the plaques when 250 μg of ^{125}I-Aβ40 was administered intravenously. Based on the pharmacokinetic parameters determined in this study, such a dose can produce plasma concentrations, at least, 50 times greater than the physiological concentrations usually observed in APP,PS1 mice. On a similar note, Selkoe and colleagues (Craft et al., 2002), based on mathematical simulations, have reported that a 100 fold reduction in plasma to brain transport of Aβ can only reduce the brain Aβ burden by less than 0.2%. These studies indicate, therefore, that plasma to brain transport of Aβ is not an important factor for plaque generation in the brain parenchyma of APP,PS1 transgenic mice. One may hypothesize, however, that very small amounts of Aβ40 transported across the BBB

over a long period of time can accumulate in high enough quantities to form plaques. This is kinetically feasible if the clearance mechanism of Aβ40 from the brains of AD mice is impaired.

The clearance of Aβ40 from the brain is known to be mediated by enzymes such as insulin degrading enzyme that metabolize the protein (Qiu et al., 1998) and the receptors (Shibata et al., 2000; Lam et al., 2001) that are involved in the efflux of the protein from CNS to plasma. Our in vitro efflux studies conducted in brain slices of 24 week old normal and APP,PS1 transgenic mice demonstrated a significantly higher rate of ^{125}I-Aβ40 efflux in the normal mice brain slices compared to the AD mice. The efflux rate decreased in the presence of 2,4-DNP (metabolic inhibitor), suggesting that ^{125}I-Aβ40 efflux across the brain slices of normal mice is carrier mediated. The lower rate of ^{125}I-Aβ40 efflux across the brain slices of APP,PS1 mice could be due to:

a) binding of ^{125}I-Aβ40 to amyloid plaques

b) impaired metabolism of ^{125}I-Aβ40

c) inefficient efflux transport

More experiments are needed to elucidate the extent each of these factors contributes to the elimination kinetics of Aβ40 from the brain.

It has been reported that Aβ40 concentration in peripheral circulation and brain exist in dynamic equilibrium, with the Aβ present in the peripheral circulation being transported to brain parenchyma to compensate for the reduction in CSF Aβ levels due to plaque formation (DeMattos et al., 2002). Similarly, Aβ from brain is transported to peripheral circulation if plasma Aβ levels are depleted due to the presence of antibodies that could sequester Aβ (DeMattos et al, 2002). Based on these studies, higher plasma

concentrations of Aβ40 in APP,PS1 animals could reduce the clearance of Aβ40 from the brain. However, our experiments demonstrated that the clearance of ^{125}I-Aβ40 from the brain is not affected by the high levels of peripheral Aβ40, suggesting once again that the influx of Aβ40 at the luminal surface of the cerebro-vascular endothelium is not significant enough to impact the capacity of the efflux transporter supposedly located on the abluminal surface.

Our studies demonstrate that the higher level of Aβ40 in the peripheral circulation in APP,PS1 mice compared to WT mice is not due to differences in the plasma, hepatic, or renal metabolism of the protein. The higher plasma concentration of exogenously added Aβ40 in WT animals inhibited the uptake of ^{125}I-Aβ40 at the BBB, but did not affect its elimination from the brain. The decreased permeability of ^{125}I-Aβ40 at the BBB in APP,PS1 animals compared to WT animals, therefore, is a direct result of higher Aβ40 levels in the plasma. Since the Aβ40 receptor at the BBB can be easily saturated, the blood-to-brain transport of Aβ40 is less likely to be a primary contributor to the amyloid plaque formation in older (6 months) APP,PS1 animals, as claimed by other investigators. The ^{125}I-Aβ40 was shown to be metabolized and effluxed in the brain parenchyma. The rate of ^{125}I-Aβ40 efflux in APP,PS1 brain slices was substantially lower compared to WT brain slices. Also, the metabolism of ^{125}I-Aβ40 was significantly lower in APP,PS1 brain slices compared to WT brain slices. Therefore, the decreased efflux of Aβ40 from the brain and its possible decreased metabolism are reasonable explanations for the Aβ accumulation and subsequent amyloid plaque formation in the brain of APP,PS1 transgenic mice. This study also demonstrates that inadequate targeting of Aβ40 to amyloid plaques despite its high BBB permeability is due to the

saturability of Aβ40 transporter at the BBB. This saturability coupled with metabolism and efflux of Aβ40 in the brain parenchyma significantly affect the plaque targeting of Aβ40. The knowledge gained from these studies is being utilized in the development of new Aβ derivatives with improved BBB permeability and plaque targeting.

REFERENCES

Cirrito JR, May PC, O'Dell MA, Taylor JW, Parsadanian M, Cramer JW, Audia JE, Nissen JS, Bales KR, Paul SM, DeMattos RB and Holtzman DM (2003) In vivo assessment of brain interstitial fluid with microdialysis reveals plaque-associated changes in amyloid-beta metabolism and half-life. *J Neurosci* **23**:8844-8853.

Craft DL, Wein LM and Selkoe DJ (2002) A mathematical model of the impact of novel treatments on the A beta burden in the Alzheimer's brain, CSF and plasma. *Bulletin of Mathematical Biology* **64**:1011-1031.

Deane R, Du Yan S, Submamaryan RK, LaRue B, Jovanovic S, Hogg E, Welch D, Manness L, Lin C, Yu J, Zhu H, Ghiso J, Frangione B, Stern A, Schmidt AM, Armstrong DL, Arnold B, Liliensiek B, Nawroth P, Hofman F, Kindy M, Stern D and Zlokovic B (2003) RAGE mediates amyloid-beta peptide transport across the blood-brain barrier and accumulation in brain. *Nat Med* **9**:907-913.

DeMattos RB, Bales KR, Parsadanian M, O'Dell MA, Foss EM, Paul SM and Holtzman DM (2002) Plaque-associated disruption of CSF and plasma amyloid-beta (Abeta) equilibrium in a mouse model of Alzheimer's disease. *J Neurochem* **81**:229-236.

Ghersi-Egea JF, Gorevic PD, Ghiso J, Frangione B, Patlak CS and Fenstermacher JD (1996) Fate of cerebrospinal fluid-borne amyloid beta-peptide: rapid clearance into blood and appreciable accumulation by cerebral arteries. *J Neurochem* **67**:880-883.

Holcomb L, Gordon MN, McGowan E, Yu X, Benkovic S, Jantzen P, Wright K, Saad I, Mueller R, Morgan D, Sanders S, Zehr C, O'Campo K, Hardy J, Prada CM,

Eckman C, Younkin S, Hsiao K and Duff K (1998) Accelerated Alzheimer-type phenotype in transgenic mice carrying both mutant amyloid precursor protein and presenilin 1 transgenes. *Nat Med* **4**:97-100.

Hsiao K, Chapman P, Nilsen S, Eckman C, Harigaya Y, Younkin S, Yang FS and Cole G (1996) Correlative memory deficits, A beta elevation, and amyloid plaques in transgenic mice. *Science* **274**:99-102.

Kuo YM, Emmerling MR, Lampert HC, Hempelman SR, Kokjohn TA, Woods AS, Cotter RJ and Roher AE (1999) High levels of circulating Abeta42 are sequestered by plasma proteins in Alzheimer's disease. *Biochem Biophys Res Commun* **257**:787-791.

Lam FC, Liu R, Lu P, Shapiro AB, Renoir JM, Sharom FJ and Reiner PB (2001) beta-Amyloid efflux mediated by p-glycoprotein. *J Neurochem* **76**:1121-1128.

Lee HJ, Zhang Y, Zhu C, Duff K and Pardridge WM (2002) Imaging brain amyloid of Alzheimer disease in vivo in transgenic mice with an Abeta peptide radiopharmaceutical. *J Cereb Blood Flow Metab* **22**:223-231.

Mackic JB, Bading J, Ghiso J, Walker L, Wisniewski T, Frangione B and Zlokovic BV (2002) Circulating amyloid-beta peptide crosses the blood-brain barrier in aged monkeys and contributes to Alzheimer's disease lesions. *Vas Pharmacol* **38**:303-313.

Matsubara E, Ghiso J, Frangione B, Amari M, Tomidokoro Y, Ikeda Y, Harigaya Y, Okamoto K and Shoji M (1999) Lipoprotein-free amyloidogenic peptides in plasma are elevated in patients with sporadic Alzheimer's disease and Down's syndrome. *Annals of Neurology* **45**:537-541.

Poduslo JF, Curran GL, Haggard JJ, Biere AL and Selkoe DJ (1997) Permeability and residual plasma volume of human, Dutch variant, and rat amyloid beta-protein 1-40 at the blood-brain barrier. *Neurobiol Dis* **4**:27-34.

Poduslo JF, Curran GL, Peterson JA, McCormick DJ, Fauq AH, Khan MA and Wengenack TM (2004) Design and chemical synthesis of a magnetic resonance contrast agent with enhanced in vitro binding, high blood-brain barrier permeability, and in vivo targeting to Alzheimer's disease amyloid plaques. *Biochemistry* **43**:6064-6075.

Poduslo JF, Curran GL, Sanyal B and Selkoe DJ (1999) Receptor-mediated transport of human amyloid beta-protein 1-40 and 1-42 at the blood-brain barrier. *Neurobiol Dis* **6**:190-199.

Poduslo JF, Curran GL, Wengenack TM, Malester B and Duff K (2001) Permeability of proteins at the blood-brain barrier in the normal adult mouse and double transgenic mouse model of Alzheimer's disease. *Neurobiol Dis* **8**:555-567.

Poduslo JF, Wengenack TM, Curran GL, Wisniewski T, Sigurdsson EM, Macura SI, Borowski BJ and Jack CR, Jr. (2002) Molecular targeting of Alzheimer's amyloid plaques for contrast-enhanced magnetic resonance imaging. *Neurobiol Dis* **11**:315-329.

Qiu WQ, Walsh DM, Ye Z, Vekrellis K, Zhang J, Podlisny MB, Rosner MR, Safavi A, Hersh LB and Selkoe DJ (1998) Insulin-degrading Enzyme Regulates Extracellular Levels of Amyloid beta -Protein by Degradation. *J Biol Chem* **273**:32730-32738.

Selkoe DJ (2001) Clearing the brain's amyloid cobwebs. *Neuron* **32**:177-180.

Shibata M, Yamada S, Kumar SR, Calero M, Bading J, Frangione B, Holtzman DM, Miller CA, Strickland DK, Ghiso J and Zlokovic BV (2000) Clearance of Alzheimer's amyloid-ss(1-40) peptide from brain by LDL receptor-related protein-1 at the blood-brain barrier. *J Clin Invest* **106**:1489-1499.

Wadghiri YZ, Sigurdsson EM, Sadowski M, Elliott JI, Li Y, Scholtzova H, Tang CY, Aguinaldo G, Pappolla M, Duff K, Wisniewski T and Turnbull DH (2003) Detection of Alzheimer's amyloid in transgenic mice using magnetic resonance microimaging. *Magn Reson Med* **50**:293-302.

Wengenack TM, Curran GL and Poduslo JF (2000a) Targeting Alzheimer amyloid plaques in vivo. *Nat Biotechnol* **18**:868-872.

Wengenack TM, Whelan S, Curran GL, Duff KE and Poduslo JF (2000b) Quantitative histological analysis of amyloid deposition in Alzheimer's double transgenic mouse brain. *Neuroscience* **101**:939-944.

Zlokovic BV (2004) Clearing amyloid through the blood-brain barrier. *J Neurochem* **89**:807-811.

Zlokovic BV, Ghiso J, Mackic JB, McComb JG, Weiss MH and Frangione B (1993) Blood-brain barrier transport of circulating Alzheimer's amyloid beta. *Biochem Biophys Res Commun* **197**:1034-1040.

Foot Notes

Address correspondence to: Dr. Joseph F. Poduslo, Mayo Clinic College of Medicine,

200 First Street SW, Rochester, Minnesota 55905. Email: poduslo.joseph@mayo.edu

30

FIGURE LEGENDS

Fig. 1A. Plasma pharmacokinetics of ^{125}I-Aβ40 in WT and APP,PS1 mice at 8 weeks. Data are mean ± S.D. (n = 3); lines indicate the fit of the two-compartment pharmacokinetic model to the plasma concentration-time data.

Fig. 1B. Plasma pharmacokinetics of ^{125}I-Aβ40 in WT (n=6) and APP,PS1 (n=3) mice at 24 weeks. Data are mean ± S.D; lines indicate the fit of the two-compartment pharmacokinetic model to the plasma concentration-time data.

Fig. 2. Degradation of ^{125}I-Aβ40 in various tissues obtained from 24 week old WT and APP,PS1 animals. Data are mean ± S.D. (n = 3).

Fig. 3. Extravascular brain uptake and plasma pharmacokinetic profile of ^{125}I-Aβ40 in 24 week old WT mice. Symbols represent observed data; line indicates the fit of the two-compartment pharmacokinetic model to the plasma concentration-time data

Fig. 4A. Effect of various doses of unlabeled Aβ40 co-administered intravenously with ^{125}I-Aβ40 (100 µCi) on the permeability of ^{125}I-Aβ40 at the blood brain barrier in 24 week old WT mice. Each result represents the mean ± S.D. for three experiments. The differences between the control (^{125}I-Aβ40) and treatments (^{125}I- Aβ40 + various amounts of unlabeled Aβ40) was determined to be statistically significant (p<0.05) by two-way ANOVA followed by Bonferroni post-tests.

31

Fig. 4B. Inhibition of ^{125}I-Aβ40 permeability at the blood brain barrier by various amounts of unlabeled Aβ40 (cold) in 24 week old WT mice. Data are mean ± S.D. (n = 3); curves represent predictions of the one-site competitive binding model.

Fig. 5. Efflux of [125]I- Aβ40 from the 24 week old WT (n=6) and APP,PS1 (n=3) brain slices in vitro; effect of 2,4-dinitrophenol on the efflux of [125]I- Aβ40 from WT brain slices. Data are mean ± S.D; curves represent predictions of the one-phase exponential decay model.

Table 1. Plasma pharmacokinetic parameters of ^{125}I-Aβ40 in wild type (WT) and APP,PS1 mice

Parameters	WT	APP, PS1	p	WT	APP, PS1	p	p†
	8 Weeks			**24 Weeks**			
C$_{max}$ (µCi/mL)	18.9 ± 2.0	10.5 ± 2.1	**	17.4 ± 2.7	14.7 ± 4.1	ns	ns
T1/2 (α) (min)	0.8 ± 0.1	0.9 ± 0.4	ns	0.9 ± 0.1	1.1 ± 0.3	ns	ns
T1/2 (β) (min)	11.9 ± 5.1	9.4 ± 6.1	ns	9.2 ± 2.3	15.0 ± 11.3	ns	ns
Clearance (ml/min/g)	0.09 ± 0.02	0.15 ± 0.02	*	0.09 ± 0.02	0.09 ± 0.02	ns	*
V$_{SS}$ (ml/g)	1.0 ± 0.3	1.4 ± 0.7	ns	0.9 ± 0.17	1.2 ± 0.76	ns	ns
AUC (min x µCi/mL)	53.0 ± 11.6	35.0 ± 4.5	*	50.5 ± 7.3	52.1 ± 9.6	ns	*

Mean ± S.D
Statistical significance was indicated by *p<0.05 and **p<0.01 using Student's t-test; ns: non-significant p > 0.05
†Comparison between 8 week and 24 week old APP,PS1 mice

33

Table 2. Saturability of various plasma pharmacokinetic parameters in 24 week old wild type mice

Parameters	Control[a] ^{125}I-Aβ40 (100μCi)	Saturation Experiments + 0.125 mg[b]	+ 0.5 mg[b]	+ 1 mg[b]	+ 2 mg[b]	+ 4 mg[b]
C_{max} (μCi/mL)	17.4 ± 2.7	21.5 ± 1.4	22.2 ± 2.5	25.3 ± 6.1	23.5 ± 7.2	21.5 ± 1.8
Clearance (ml/min)	2.0 ± 0.3	1.6 ± 0.4	1.3 ± 0.4	1.3 ± 0.2	1.0 ± 0.2**	0.7 ± 0.3**
V_{SS} (ml)	17.1 ± 3.7	16.6 ± 0.3	14.1 ± 1.8	9.6 ± 2.9*	9.1 ± 2.1**	11.6 ± 2.6*
AUC (min x μCi/mL)	50.5 ± 7.3	65.3 ± 17.9	83.0 ± 22.0	77.6 ± 15.5	100.6 ± 28.6	163.7 ± 76.6**

Mean ± S.D
[a]Control experiments were performed by administering a 100 μCi bolus dose of ^{125}I-Aβ40 intravenously
[b]Indicate the amount of unlabeled Aβ40 administered intravenously with 100 μCi of ^{125}I-Aβ40
Statistical significance was indicated by *p<0.05 and **p<0.01 using one-way ANOVA; ns: non-significant p > 0.05

Table 3. Effect of various amounts of Aβ40 on the PS and V_p values of ^{125}I-Aβ40 at the BBB of wild type mice (24 weeks)

Brain Region	^{125}I-Aβ40	^{125}I-Aβ40 + 0.125 mg Aβ40	^{125}I-Aβ40 + 0.5 mg Aβ40	^{125}I-Aβ40 + 1mg Aβ40	^{125}I-Aβ40 + 2 mg Aβ40	^{125}I-Aβ40 + 4 mg Aβ40
PS (ml/g/s x10^{-6})						
Cortex	111.9 ± 6.0	78.4 ± 19.5	52.3 ± 8.9	39.5 ± 8.7	29.9 ± 2.9	24.1 ± 4.1
Caudate-putamen	129.5 ± 13.4	65.6 ± 18.7	45.1 ± 10.4	36.3 ± 6.1	23.3 ± 2.3	18.2 ± 3.3
Hippocampus	119.6 ± 13.0	79.6 ± 3.4	63.0 ± 15.7	45.1 ± 12.5	28.8 ± 2.5	29.1 ± 4.9
Thalamus	128.4 ± 13.4	96.2 ± 22.0	54.9 ± 8.5	44.8 ± 12.7	31.0 ± 3.8	32.6 ± 9.8
Brain stem	133.9 ± 13.5	103.5 ± 34.3	68.1 ± 11.5	52.4 ± 19.3	40.1 ± 2.0	35.0 ± 7.7
Cerebellum	135.7 ± 20.8	99.8 ± 18.6	67.2 ± 14.5	53.4 ± 23.8	39.7 ± 2.2	33.9 ± 7.7
V_p (µl/g)						
Cortex	18.1 ± 1.3	19.8 ± 2.3	16.6 ± 1.9	17.6 ± 3.0	20.8 ± 2.1	18.9 ± 1.2
Caudate-putamen	13.5 ± 2.2	11.2 ± 1.5	9.9 ± 0.5	11.4 ± 2.4	11.3 ± 2.5	10.0 ± 0.5
Hippocampus	18.2 ± 2.8	18.0 ± 4.3	18.2 ± 4.6	17.5 ± 0.4	18.7 ± 2.2	18.3 ± 3.8
Thalamus	18.6 ± 2.4	20.9 ± 4.8	15.3 ± 1.4	16.3 ± 1.6	17.8 ± 1.8	18.6 ± 2.1
Brain stem	23.3 ± 2.4	27.4 ± 6.4	20.3 ± 1.1	25.4 ± 4.1	29.9 ± 0.4*	25.8 ± 6.1
Cerebellum	23.0 ± 1.3	26.5 ± 3.4	19.9 ± 3.6	22.3 ± 4.2	27.3 ± 1.3*	25.1 ± 2.4

Mean ± S.D. According to two-way ANOVA followed by Bonferroni post-tests, PS values obtained after the co-administration of various amounts of Aβ40 are significantly different ($p < 0.05$) from that of ^{125}I-Aβ40. Whereas, V_p values obtained after the co-administration of various amounts of Aβ40 are not significantly different from that of ^{125}I-Aβ40 values except those denoted by *($p > 0.05$).

Table 4. PS and V_p of Aβ40 at the BBB in wild type (WT) and APP, PS1 transgenic mice

Brain Region	WT	APP, PS1	p	APP, PS1/ WT	WT	APP, PS1	p	APP, PS1/ WT
	8 weeks				24 weeks			
PS (ml/g/s x10^{-6})								
Cortex	107.3 ± 13.9	68.5 ± 4.9	**	0.6	111.9 ± 6.0	63.4 ± 16.7	**	0.5
Caudate-putamen	87.1 ± 10.1	63.7 ± 18.0	ns	0.7	129.5 ± 13.4	46.9 ± 13.0	***	0.4
Hippocampus	96.9 ± 3.7	60.8 ± 5.6	**	0.6	119.6 ± 13.0	82.4 ± 21.7	*	0.7
Thalamus	120.3 ± 7.5	78.9 ± 15.8	**	0.7	128.4 ± 13.4	67.8 ± 21.9	***	0.5
Brain stem	127.0 ± 13.3	93.7 ± 6.9	**	0.7	133.9 ± 13.5	82.4 ± 8.1	**	0.6
Cerebellum	128.3 ± 14.2	80.5 ± 12.7	***	0.6	135.7 ± 20.8	76.9 ± 19.3	***	0.5
V_p (µl/g)								
Cortex	18.6 ± 2.2	17.8 ± 1.6	ns	1.0	18.4 ± 1.6	21.2 ± 0.5	ns	1.1
Caudate-putamen	10.9 ± 2.5	11.3 ± 2.9	ns	1.0	14.9 ± 1.2	11.6 ± 1.5	ns	0.8
Hippocampus	14.3 ± 1.0	13.9 ± 0.8	ns	1.0	18.0 ± 3.1	25.8 ± 0.9	**	1.4
Thalamus	19.8 ± 2.0	19.5 ± 3.0	ns	1.0	18.9 ± 3.1	18.3 ± 2.1	ns	1.0
Brain stem	24.1 ± 3.8	24.7 ± 2.2	ns	1.0	22.9 ± 3.0	30.7 ± 6.7	**	1.3
Cerebellum	23.1 ± 2.8	20.7 ± 1.2	ns	1.0	23.1 ± 1.7	26.7 ± 2.2	ns	1.1

Mean ± S.D
Statistical significance was indicated by *$p<0.05$, **$p<0.01$ and ***$p<0.001$ using Student's t-test; ns: non-significant $p > 0.05$

Table 5. Comparison of extravascular content and V_p values of ^{125}I-Aβ40 resulting from multiple dosing experiments in 24 week old WT mice

Brain Region	Control	Treatment	p
Extravascular ^{125}I- Aβ40 (cpm/mg)			
Cortex	242 ± 60	217 ± 15	ns
Caudate-putamen	223 ± 25	181 ± 18	ns
Hippocampus	273 ± 52	288 ± 51	ns
Thalamus	275 ± 55	250 ± 61	ns
Brain stem	379 ± 98	370 ± 76	ns
Cerebellum	387 ± 50	310 ± 37	ns
V_p (µl/g)			
Cortex	16.3 ± 8.3	17.6 ± 1.2	ns
Caudate-putamen	10.9 ± 5.1	10.4 ± 1.2	ns
Hippocampus	16.7 ± 8.0	18.9 ± 3.6	ns
Thalamus	14.8 ± 5.3	18.0 ± 3.7	ns
Brain stem	23.6 ± 10.7	26.7 ± 6.7	ns
Cerebellum	24.6 ± 12.3	23.1 ± 5.4	ns

According to Student's t-test, there is no statistically significant (ns; $p > 0.05$) difference between the control and the treatment.

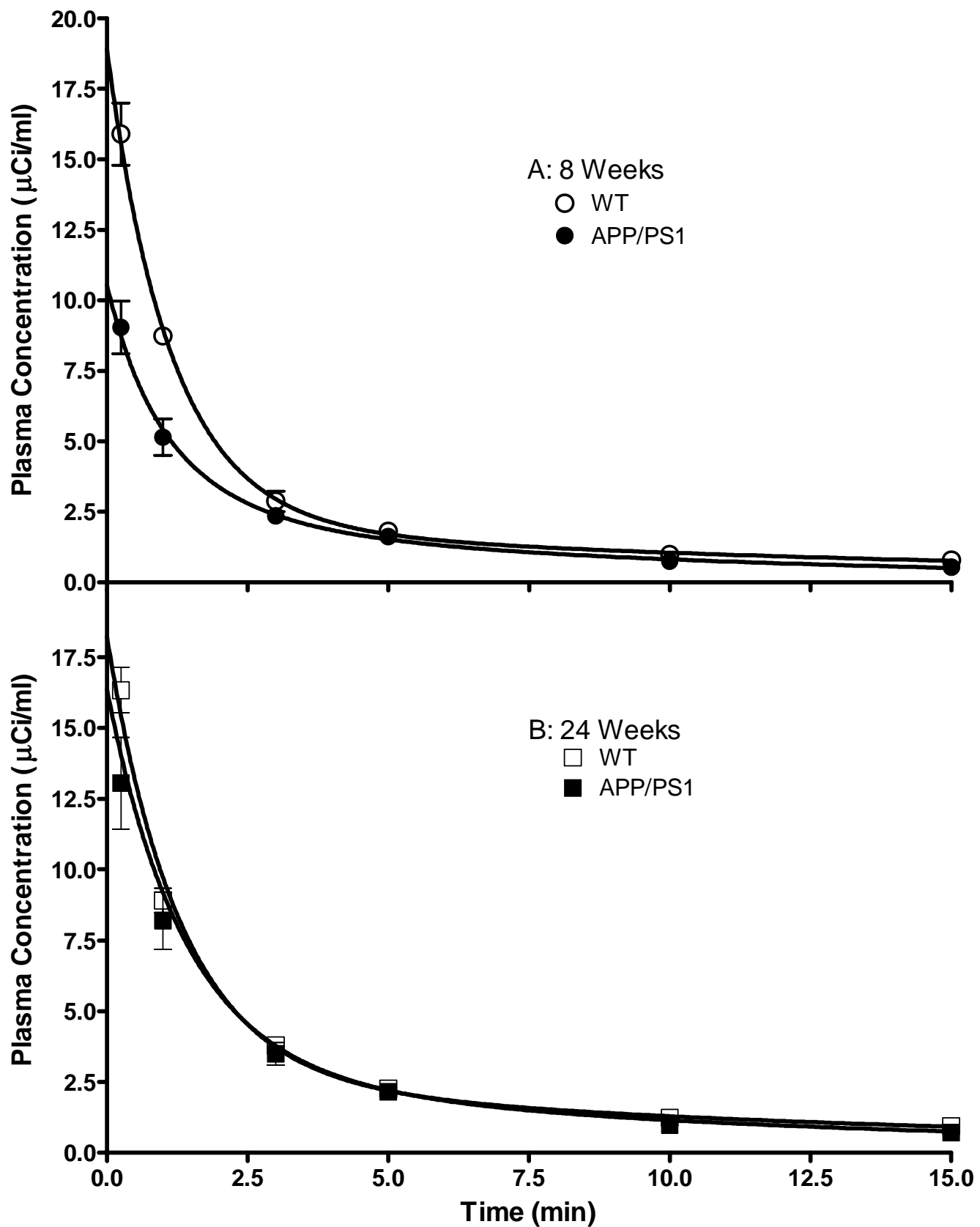**Figure 1**   **JPET #81901**
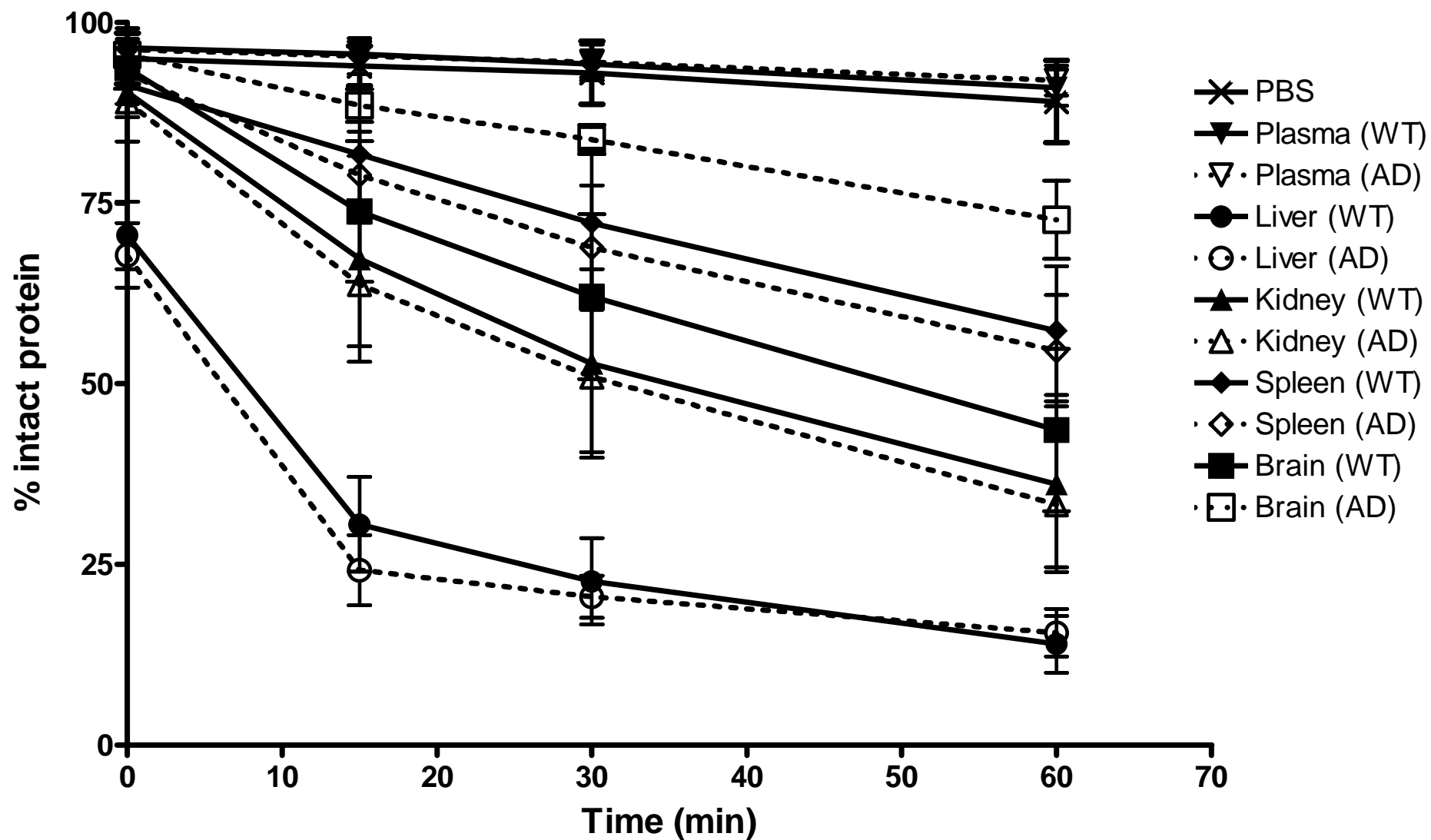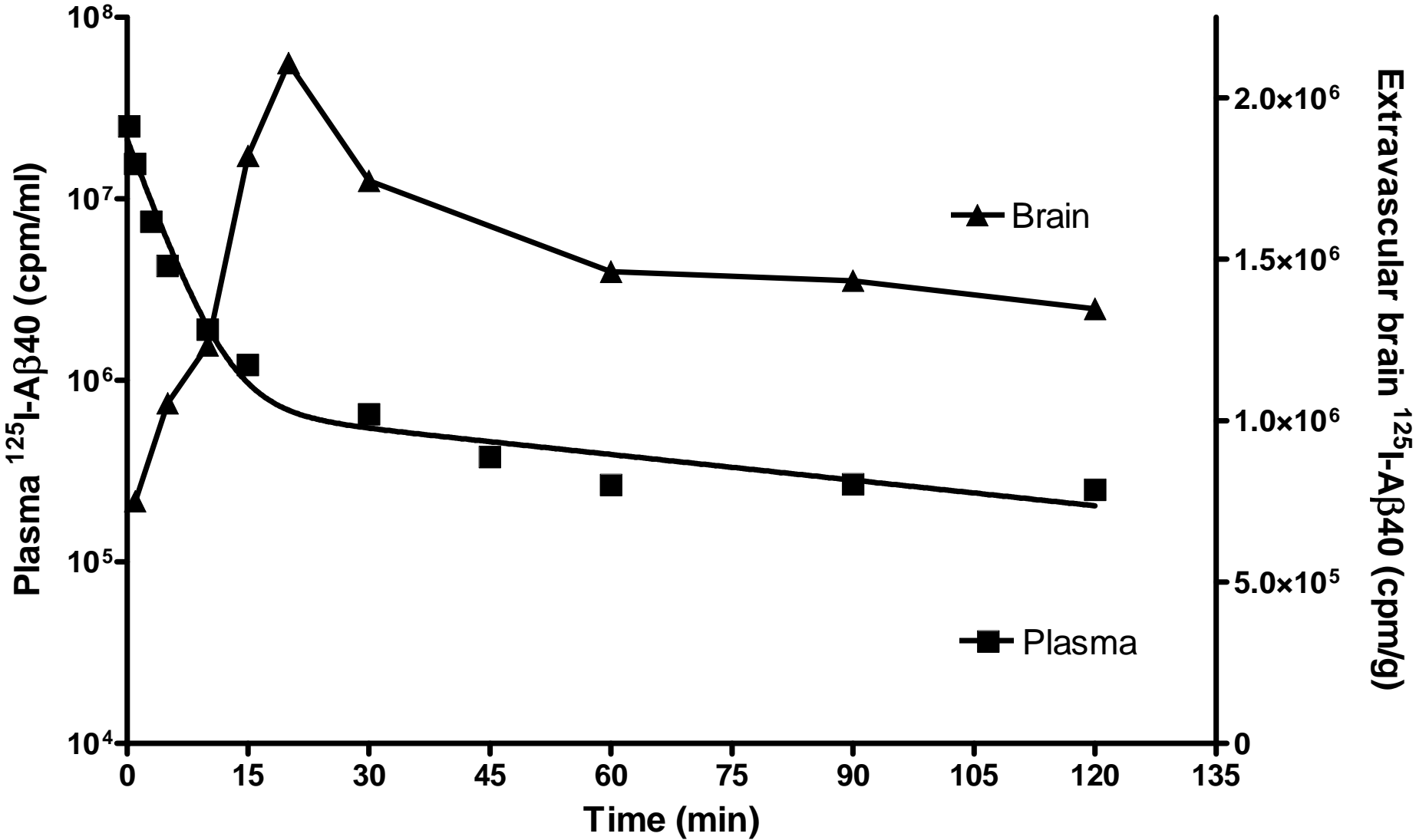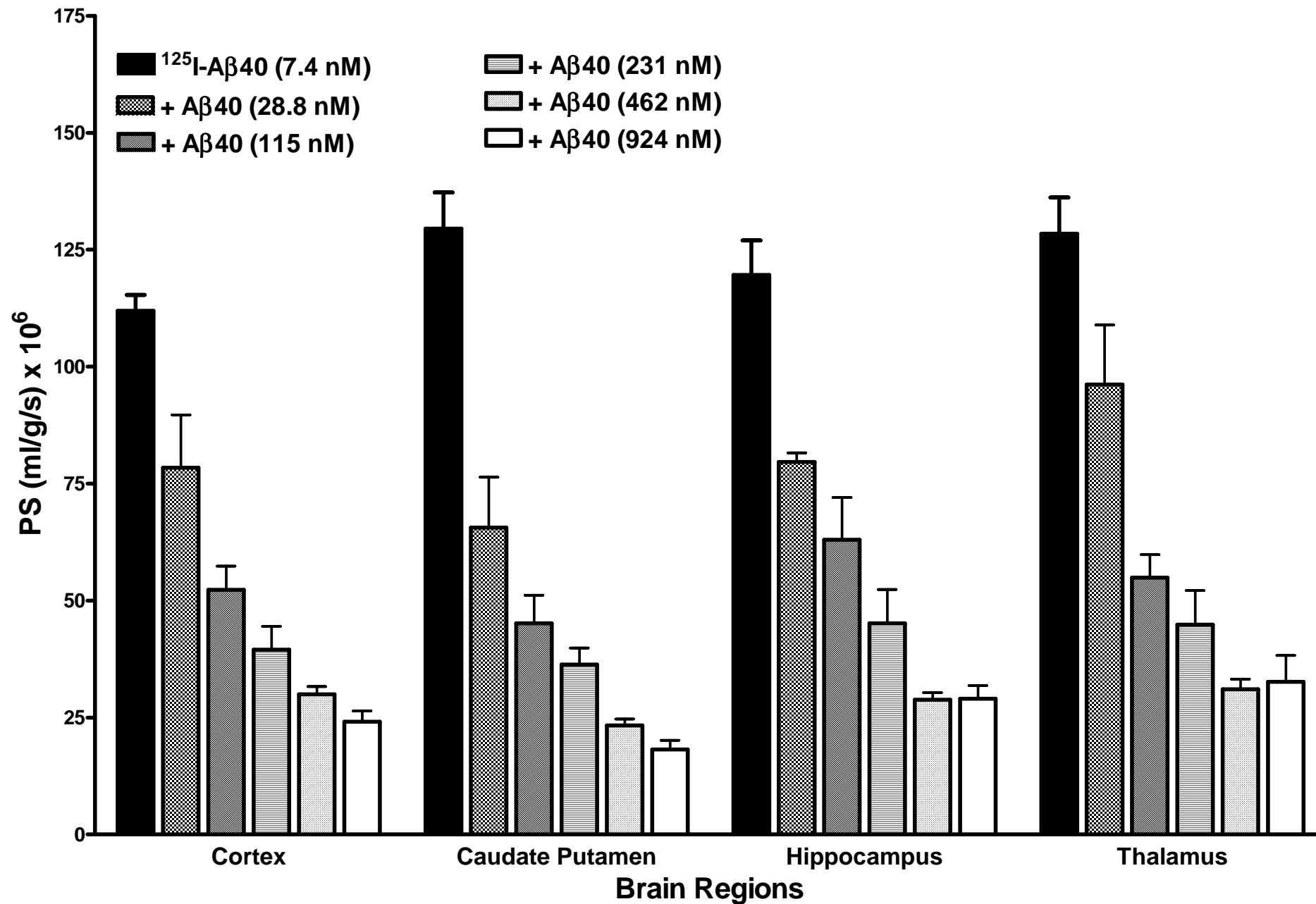
Figure 2   **JPET #81901**

Figure 3 **JPET #81901**

Figure 5

JPET #81901